Earth's Future

RESEARCH ARTICLE
10.1029/2022EF002674

Special Section:
CMIP6: Trends, Interactions, Evaluation, and Impacts

The Carbon Sink Potential of Southern China After Two Decades of Afforestation

X. M. Zhang[1,2,3], M. Brandt[4], Y. M. Yue[1,2], X. W. Tong[1,4], K. L. Wang[1,2], and R. Fensholt[4]

[1]Guangxi Key Laboratory of Karst Ecological Processes and Services, Institute of Subtropical Agriculture, Chinese Academy of Sciences, Changsha, China, [2]Huanjiang Observation and Research Station for Karst Ecosystem, Chinese Academy of Sciences, Huanjiang, China, [3]University of Chinese Academy of Sciences, Beijng, China, [4]Department of Geosciences and Natural Resource Management, University of Copenhagen, Copenhagen, Denmark

Abstract Afforestation and land use changes that sequester carbon from the atmosphere in the form of woody biomass have turned southern China into one of the largest carbon sinks globally, which contributes to mitigating climate change. However, forest growth saturation and available land that can be forested limit the longevity of this carbon sink, and while a plethora of studies have quantified vegetation changes over the last decades, the remaining carbon sink potential of this area is currently unknown. Here, we train a model with multiple predictors characterizing the heterogeneous landscapes of southern China and predict the biomass carbon carrying capacity of the region for 2002–2017. We compare observed and predicted biomass carbon density and find that during about two decades of afforestation, 2.34 PgC have been sequestered between 2002 and 2017, and a total of 5.32 Pg carbon can potentially still be sequestrated. This means that the region has reached 73% of its aboveground biomass carbon carrying capacity in 2017, which is 12% more than in 2002, equal to a decrease of 0.77% per year. We identify potential afforestation areas that can still sequester 2.39 PgC, while old and new forests have reached 87% of their potential with 1.85 PgC remaining. Our work locates areas where vegetation has not yet reached its full potential but also shows that afforestation is not a long-term solution for climate change mitigation.

Plain Language Summary Forests sequester carbon dioxide from the atmosphere in the form of vegetation biomass, and tree planting initiatives are thus suggested as a promising measure against climate change. China has recently planted millions of trees, which sequester large amounts of carbon, but this carbon sink is not infinite. We quantify the amount of carbon that can still be sequestered in the forests of southern China. We find that 73% of the limits have been reached in 2017, which is 12% more than in 2002, when the tree planting initiatives started. This illustrates that planting trees is only a short term solution and only a reduction of CO_2 emissions helps to mitigate climate change in the long term.

Key Points:

- We estimate the aboveground forest biomass of southern China to be 15.22 PgC in 2017 and the carrying capacity is 20.54 PgC
- Afforestation starting in 2002 has consumed 2.34 PgC, but 5.32 PgC of potential carbon sinks are left
- Afforestation approaches the carbon sink limits quickly and is not a long term measure to achieve carbon neutrality

Supporting Information:

Supporting Information may be found in the online version of this article.

Correspondence to:

Y. M. Yue,
ymyue@isa.ac.cn

Citation:

Zhang, X. M., Brandt, M., Yue, Y. M., Tong, X. W., Wang, K. L., & Fensholt, R. (2022). The carbon sink potential of southern China after two decades of afforestation. *Earth's Future*, *10*, e2022EF002674. https://doi.org/10.1029/2022EF002674

Received 26 JAN 2022
Accepted 4 NOV 2022

Author Contributions:

Conceptualization: X. M. Zhang, M. Brandt, X. W. Tong, K. L. Wang
Data curation: X. M. Zhang, X. W. Tong
Formal analysis: X. M. Zhang, M. Brandt
Funding acquisition: M. Brandt, Y. M. Yue, X. W. Tong, K. L. Wang

1. Introduction

Global warming, resulting from human-induced emissions of greenhouse gases, not only increases the frequency of extreme climate events and causes the sea level to rise (Benítez et al., 2007; IPCC, 2001), but also leads to adverse environmental impacts, such as the reduction of vegetation productivity and biodiversity (Wu et al., 2021), significant losses of soil inorganic carbon (X. D. Song et al., 2021), and the disturbance of the natural carbon cycle (Reichstein et al., 2013). Forests sequester carbon dioxide from the atmosphere in the form of vegetation biomass, and are thus an effective way to reduce atmospheric carbon (Nunes et al., 2020; Zhang, Yue, et al., 2021). The total global forest carbon stock is estimated to be 662 PgC, of which ~45% is stored in living aboveground biomass (FAO, 2020), accounting for 70%–90% of the total living biomass carbon of the world's major terrestrial ecosystem (Houghton, 2008). With increasing greenhouse gas emissions, reports such as the United Nations Framework Convention on Climate Change propose to invest in afforestation to remove carbon dioxide from the atmosphere. The regrowth of natural forests is considered as one of the most important natural climate solutions (Cook-Patton et al., 2020).

China has invested considerable effort in increasing vegetation coverage by forestation projects (Fang et al., 2018). By 2020, China has afforested a total of 6.77 million hectares (FAO, 2020; SFGA, 2021) leading to a total forest area of 220 million hectares, which accounts for 5% of the global forests (FAO, 2020). About 45% of these forests are concentrated in and around the karst region of southern China (Tong et al., 2020), making this area

Investigation: X. M. Zhang, M. Brandt
Methodology: X. M. Zhang, M. Brandt
Project Administration: M. Brandt, Y. M. Yue, X. W. Tong, K. L. Wang, R. Fensholt
Resources: M. Brandt, Y. M. Yue, X. W. Tong, R. Fensholt
Software: X. M. Zhang, M. Brandt
Supervision: M. Brandt, Y. M. Yue, X. W. Tong, K. L. Wang, R. Fensholt
Validation: X. M. Zhang, M. Brandt
Visualization: X. M. Zhang, M. Brandt
Writing – original draft: X. M. Zhang
Writing – review & editing: X. M. Zhang, M. Brandt, Y. M. Yue, X. W. Tong, K. L. Wang, R. Fensholt

a global hot spot of vegetation growth (Brandt et al., 2018; Tong et al., 2018). Indeed, Tong et al. (2020) have shown that land and forest management have removed an amount of carbon equivalent to 33% of the regional fossil fuel emissions over the last decade. Following massive plantation efforts, the forest growth of this area was remarkable (Tong et al., 2020), yet many studies indicate that carbon storage increases quickly in young forests, but reaches a relatively stable level in older forests (He et al., 2017; Wang et al., 2011; Yu et al., 2017; Zhang et al., 2017). Moreover, forest growth and carbon storage potential of the region are heterogeneous, depending on land use, forest stand age and type, as well as landscape and climate (Brandt et al., 2018; Cai et al., 2021; He et al., 2017; Y. C. Liu et al., 2014, H. Y. Liu et al., 2020; Tong et al., 2020). Consequently, while CO_2 emissions continue to increase, estimating the remaining carbon removal potential of southern China's forests is important for ecological restoration strategies.

Estimating the potential of a forest to sequester carbon requires comparing its current state with its carbon carrying capacity, which is the amount of carbon that can be stored in forests under prevailing environmental conditions and natural disturbance regimes (Keith et al., 2010; Roxburgh et al., 2006). Forest surveys and field observations are widely used to estimate the carbon sequestration capacity under different growing and management scenarios (Cai et al., 2021; Kumar. 2006; Lal & Singh, 2000; Macreadie et al., 2017; Roxburgh et al., 2006; Tang et al., 2018; Udawatta & Jose, 2011). Y. C. Liu et al. (2014) estimated the carbon carrying capacity in China based on 338 forest inventory sites in 2006, 2007, and 2010, and calculated a carrying capacity of 19.87 PgC with a remaining potential of 13.86 PgC. Cai et al. (2021) used the forest carbon sequestration model from 3,365 forest survey plots, to assess the carbon sequestration rate of Chinese existing and new forests during 2010–2060. They found a carbon sequestration rate of 0.21 PgC yr^{-1} over the period, with 11% of this sink coming from forestation. However, the application of these assessments based on field records in areas characterized by spatially heterogeneous landscapes and with a high forest dynamic, like southern China, is challenging.

Multi-source satellite data and machine learning allow for a rapid assessment of aboveground biomass carbon sequestration potentials at global and regional scales (Hamilton & Friess, 2018; Pascual et al., 2021; Ross et al., 2021). The prediction of the carbon sink potential is particularly important in forest plantation areas, such as in some parts of the Brazilian Amazon (Heinrich et al., 2021), the Hawaiian forest reserves (Pascual et al., 2021), or the Three-North Shelterbelt in China (Zhang et al., 2021). This is also the case for southern China, where a heterogeneous landscape impedes generalized assumptions and requires locally calibrated models. A high level of details, including different land covers/uses, human disturbances as well as long-term observations covering larger areas are important to provide a scientific reference for regional policymakers and stakeholders evaluating and planning ecological protection measures.

Many studies have verified that climatic and geological settings impact vegetation growth (H. Y. Liu et al., 2020; Piao et al., 2015; Zhang et al., 2021; Zhao et al., 2020). Based on these studies, here we used 17 environmental factors (6 climate factors and 11 natural geological factors) (Table S1 in Supporting Information S3) well describing the local landscape characteristics to predict the carbon carrying capacity of southern China modeled at a 500 × 500 m resolution. We derived the per-pixel carbon sink potential by comparing the carbon carrying capacity with the observed carbon density (data set available from Tong et al. (2020)) per grid cell for the years 2002–2017. We used annual forest maps to monitor changes in the carbon sink potential of old forests (always forest over 2002–2017), new forests (no forest in 2002 but in 2017) and potential forests (never forest over 2002–2017), and study the remaining aboveground woody biomass carbon sink potential in 2017. The major objectives of this study were to assess to what extend forest growth has reached the limits of the carbon sink potential of southern China over 2002–2017, to quantify the remaining carbon sink potential for different forest types in 2017, and to determine which factors influence the spatial patterns.

2. Materials and Methods

2.1. Study Area

The study area (Figure 1) is located in southern China and covers over 1.96 million km^2, including the provinces Hubei, Hunan, Guangdong, Guangxi, Guizhou, Yunnan, Sichuan, and Chongqing. The sloping landscape is characterized by a variety of different karst formations, large variations in mean annual temperature (MAT) (−14°C to 25°C) and rainfall (518–2,235 mm), and decades of deforestation followed by decades of afforestation. Urbanization, rural depopulation, and ecological protection programs have reduced the agricultural use of

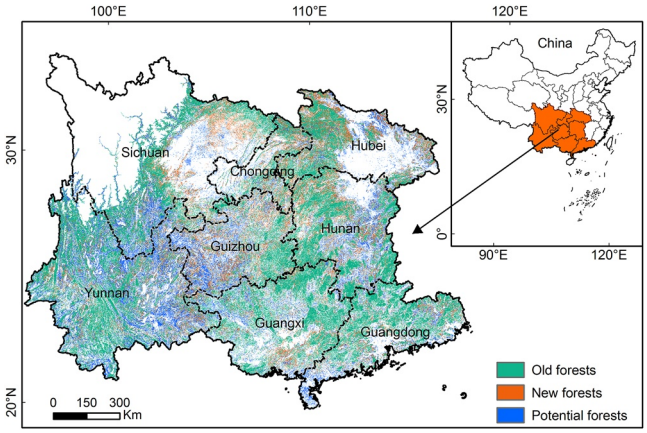

Figure 1. Study area and forest types. Annual forest data are from Tong et al. (2020). Old forests were forests during 2002–2017, new forests were forests in 2017 but not in 2002, and potential forests have not been forested during 2002–2017. Croplands, urban areas and the Southeast margin of the Tibetan Plateau have been masked. The masked areas are shown in white.

the area, with about 29% still being croplands in 2020. A total of 28% of the region are covered by karst, which are often degraded landscapes subject to various ecological projects (Wang et al., 2019). A total of 32% of the study region are covered by urban areas and croplands, of which most (71%) are found in the non-karst area. Other major vegetation types are subtropical evergreen and deciduous broad-leaved forests (~50%) and grassland (~14%) (Wang et al., 2019). The Southeast margin of the Tibetan Plateau has an annually accumulated temperature with days ≥10°C (°C-days) lower than 2000°C and is not suited for forests, so we masked this area in our study (CMA, 1978). We also masked croplands and urban areas (32% of the study area) as a reduction of croplands on the expense of additional afforestation would lead to unpredictable shortages in the food production. Croplands, urban and water areas were masked using the maps from Globeland30 from 2020 (30 × 30 m) (http://www.globeland30.org/).

2.2. Annual C Density and Forest Probability Maps

Both the annual carbon density and annual forest maps are available at a resolution of 500 × 500 m for 2002–2017 from Tong et al. (2020). The annual carbon density of the study area shows aboveground woody biomass and uses boosted regression trees, which were trained with a static global benchmark map of carbon density of woody vegetation for 2018, using MODIS (MCD43A4 7 bands; NDII, EV12, MCD43A3 shortwave albedo) and STRM data. We refer to Tong et al. (2020) for details on the maps.

We used the annual (2002–2017) forest probability maps from Tong et al. (2020) which were also derived from MODIS data. A probability threshold of 0.5 was used to define if an area is a forest or not (Tong et al., 2020). We identified three types of forests (Figure 1): (a) old forests (always forest during 2002–2017), (b) new forests (no forest in 2002 but in 2017), and potential forests (never forested during 2002–2017). Note that potential forests may include areas where forest growth is limited by natural factors, which is reflected by the 17 environmental factors (Section 2.4).

2.3. Environmental Data and the Human Influence Intensity Index

We used 17 environmental factors (Table S1 in Supporting Information S3) to predict the potential carbon density: MAT (°C), mean annual precipitation (mm, MAP), annually accumulated temperature with days ≥0°C (°C-days, AAT0), annually accumulated temperature with days ≥10°C (°C-days, AAT10), aridity index and humidity index. These data are available from the Research Center for Eco-Environmental Sciences, Chinese Academy of Sciences (https://www.resdc.cn/). Further data applied are maps on the lithology, geology (China Geological Survey) (Pang et al., 2017), and the hydrological richness (obtained by summing the hydrological elements from the 1:1M scale national fundamental geographic map including rivers, lakes and springs) (https://www.webmap.cn/) (Figure S1 in Supporting Information S2) (Lv et al., 2019), as well as geomorphological units (Cheng & Zhou, 2014), topography (Digital Elevation Model (DEM), slope, aspect) and soil properties (soil types, clay content, sand content and silt content) (https://www.resdc.cn/).

The human influence intensity (HII) index proposed by Sanderson et al. (2002) was used. We applied a road distance map (https://www.openstreetmap.org/), a grided population density map from 2015 (1 × 1 km) (https://www.resdc.cn/), nighttime lights from 2018 (500 × 500 m) (https://dataverse.harvard.edu/) (Chen et al., 2020) and land use data from 2020 (30 × 30 m) (http://www.globeland30.org/) to generate the HII at 500 × 500 m. We assigned scores to population density, roads and railways, land use/cover, which were summed to quantify the HII, which ranges from 0.05 to 30 (Text S1 in Supporting Information S1).

2.4. Predicting the Carbon Carrying Capacity

We selected all pixels with a carbon density value above the 75% quantile of each province resulting in a total number of 728,786 pixels. The stratification in provinces guarantees that diverse landscapes are covered (Table

S2 in Supporting Information S3). Selecting only high values assumes that vegetation in these areas has reached a mature state representing values close to the carbon carrying capacity. Out of these values, we randomly selected 50,000 samples that were used to train a Random Forest model. The 17 environmental factors (previous section) were used as independent variables to predict the carbon carrying capacity for each 500 × 500 m pixel. The per-pixel prediction reflects the carbon carrying capacity of individual factor combinations. To guarantee a robust model, we repeated the procedure 5 times with different random samples, thereby training 5 separate models. We used the average of the 5 models for the presentation of the results, and the difference between the models reflects the uncertainty. The average R^2 of the models was 0.92 and the average PMSE was 22.75 Mg C ha^{-1} and, MAE 15.12 Mg C ha^{-1} (Table S3 in Supporting Information S3).

The difference between observed carbon density and the carbon carrying capacity is the potential carbon density. The observed carbon stocks/carbon carrying capacity in % shows how much of the carrying capacity has been reached during 2002–2017. Low percentage values imply that the area has not reached its carbon carrying capacity (corresponding to 100%). Note that the carbon carrying capacity is predicted per pixel using the 17 factors; this reflects the local environment and leads to realistic estimations given the local conditions. If an area is not suited for forests, the predicted carbon carrying capacity will be low.

2.5. The Optimal Parameter-Based Geographical Detector (OPGD) Model

Identifying the potential constraints of forest growth in regions with different natural conditions and human activities is crucial to optimize actions to achieve the local carbon carrying capacity. The OPGD model consists of five parts: the factor detector, parameter optimization, the interaction detector, the risk detector, and the ecological detector (Y. Z. Song et al., 2020).

The factor detector, the core part of the OPGD model, was used to explore the relative importance of factors influencing the spatial patterns of carbon density using a Q statistic (Y. Z. Song et al., 2020; Wang & Xu, 2017). The Q statistic of each factor v is calculated as follows:

$$Q_v = \frac{\sum_{i=1}^{L} N_{v,i}\sigma_{v,i}^2}{N_v\sigma_v^2}$$

Where $N_{v,i}$ and $\sigma_{v,i}^2$ represent the number and the variance of C density in ith ($i = 1, \ldots, L$) stratum of factor v; N_v and σ_v^2 represent the number and the variance of C density over the entire study area. The F-test is used to determine significant ($p < 0.05$) differences among the stratified factors.

Based on the factor detector, the interaction detector can explore whether the influence of a spatial interaction of two overlapping spatial factors on carbon density is weakened, enhanced or independent by comparing the relative importance (Q values) of the interactions and individuals (Table S4 in Supporting Information S3). The ecological detector can also be used to test the significance of the differences between Q values based on the F-statistic (Wang & Xu, 2017).

Regarding the parameters optimization, the parameter combination with the highest Q value was selected to determine the most suitable discretization method and stratum numbers (L) of the continuous factors (Text S2 in Supporting Information S1). For the HII, we used 5 levels (Figure S2 in Supporting Information S2): slight pressure ($0.05 < \text{HII} \leq 9.67$), light pressure ($9.67 < \text{HII} \leq 11.20$), moderate pressure ($11.20 < \text{HII} \leq 14.84$), severe pressure ($14.84 < \text{HII} \leq 18.95$), and extreme pressure ($18.95 < \text{HII} \leq 30$), based on the optimal parameter combination of the OPGD model (Table S5 in Supporting Information S3) and previous studies (S. C. Li et al., 2018; Nguyen & Liou, 2019). Similarly, it was also used for rainfall, temperature, slope (Yue et al., 2020) and DEM (B. Y. Li et al., 2008) (Figure S3 in Supporting Information S2).

The risk detector can show the mean values of predicted, observed and potential carbon density in each stratified factors, used to search for areas with high observed and potential carbon density. The differences between mean values of subregions can be compared using a t-test (Wang & Xu, 2017).

3. Results

3.1. Changes of Potential Carbon Stocks

We calculated the difference between the predicted biomass carbon carrying capacity, and the observed biomass carbon stocks to reflect the potential carbon stocks, which is the amount of carbon that can potentially still be sequestered in biomass. The potential carbon stocks were calculated for the period 2002–2017. Note that we did not include croplands and urban areas in these calculations. Our results show that forestation and associated carbon density gains decreased the remaining potential carbon density from 65.97 ± 2.60 MgC ha^{-1} in 2002 to 45.79 ± 2.60 MgC ha^{-1} in 2017, which is a decrease of −30.69% (Figure 2b). More specifically, only 10.19% of the entire area has reached a saturated stage during the period, while 49.21% remain below their potential. This implies that 12.88 PgC had been sequestered before 2002, 2.34 PgC during 2002–2017, and 5.32 ± 0.30 PgC can still be sequestrated. In other words, 61.14 ± 1.46% of the carbon carrying capacity was reached in 2002, while it is 73.45 ± 1.46% in 2017 (Figure 2c). Most carbon gains were observed in the mountains around the Chengdu Plain, as well as the karst regions of western Hubei, Hunan, Guizhou, and Guangxi (Figure 2a). The center of the Yunnan-Guizhou Plateau (eastern Yunnan, Guizhou, and northwestern Guangxi) has the largest remaining carbon sink potential, highlighting this region as a target area for future ecological restoration projects, but also eastern Hunan and Hubei show a considerable remaining potential (Figure 2a). The potential carbon stocks continuously declined from 2002 to 2017 with 0.15 PgC $year^{-1}$, following a polynomial fit (Figure 2c). If the forest growth continues following this fit, the carbon carrying capacity would possibly be reached around 2030.

3.2. Carbon Sequestration Potential for Different Forest Types

We used annual forest maps generated by Tong et al. (2020) to classify the study area into old forests (always forest during 2002–2017), new forests (no forest in 2002, but in 2017) and potential forests (never forest during 2002–2017). Potential forests, new forests, and old forests account for 10.91%, 8.23%, and 23.51% of the study area (Figure 1 and 3a). All three types show an overall decrease in potential carbon stocks over 2002–2017, implying that the observed carbon stocks are increasing (Figures 3b–3d). The strongest decrease of potential carbon density was found in new forests (2.59 ± 0.15 MgC ha^{-1} yr^{-1}, 25.26 ± 1.42%), followed by potential forests (1.13 ± 0.18 MgC ha^{-1} yr^{-1}, 10.86 ± 1.58%) and old forests (0.90 ± 0.18 MgC ha^{-1} yr^{-1}, 8.60 ± 1.48%) (Figures 3b and 3d). In 2017, potential forests have reached 43.06 ± 1.58% of their carbon carrying capacity, with 2.39 ± 0.07 PgC (100.15 ± 2.87 MgC ha^{-1}) potential carbon stocks remaining. New forests have reached 71.01 ± 1.42% with 0.86 ± 0.04 PgC (47.84 ± 2.44 MgC ha^{-1}) remaining, and old forests have reached 88.82 ± 1.48% with 0.99 ± 0.15 PgC (19.21 ± 2.90 MgC ha^{-1}) remaining. The potential carbon stocks decreased at the same rate in new forests (0.05 ± 0.003 PgC yr^{-1}) and old forests (0.05 ± 0.01 PgC yr^{-1}), followed by potential forests (0.03 ± 0.004 PgC yr^{-1}) (Figure 3d). Overall, 9.75×10^4 km^2 (4.99%) of the area has reached their carbon carrying capacity within the three forest types during the period: 12.31% (1.20×10^4 km^2) of the new forests and 84.92% (8.28×10^4 km^2) of the old forests (Figure 3c). Non-karst areas showed a stronger decrease of potential carbon density in new forests (2.74 ± 0.16 MgC ha^{-1} yr^{-1}) as compared to karst areas (2.34 ± 0.14 MgC ha^{-1} yr^{-1}), but the values in old forests in karst area (1.04 ± 0.17 MgC ha^{-1} yr^{-1}) decreased faster than in non-karst areas (0.85 ± 0.18 MgC ha^{-1} yr^{-1}).

3.3. Factors Influencing Potential and Observed Carbon Density

We applied a factor detection (Q-value) to explore the drivers influencing potential and observed carbon density in southern China; note that croplands and urban areas are excluded (Figure 4). The results show that the geographical setting is the major factor explaining the spatial patterns. With a Q value of 0.11, the terrain relief had the strongest influence on the spatial pattern of the potential carbon density, followed by soil types and slope, both with a Q value of 0.06. The observed carbon density was most influenced by elevation, with a Q value of 0.40. Climate conditions impact both potential and observed carbon density. MAP mostly influenced the potential carbon density but not the observed carbon density, while it was the opposite for MAT. In addition, even though we excluded croplands and urban areas, the human influence factor had a clear influence on the spatial patterns of potential and observed carbon density, with Q values of 0.09 and 0.14, respectively. The influence of soil types on potential carbon density was almost the same as climate zones (0.06), but was stronger on observed carbon density (0.15).

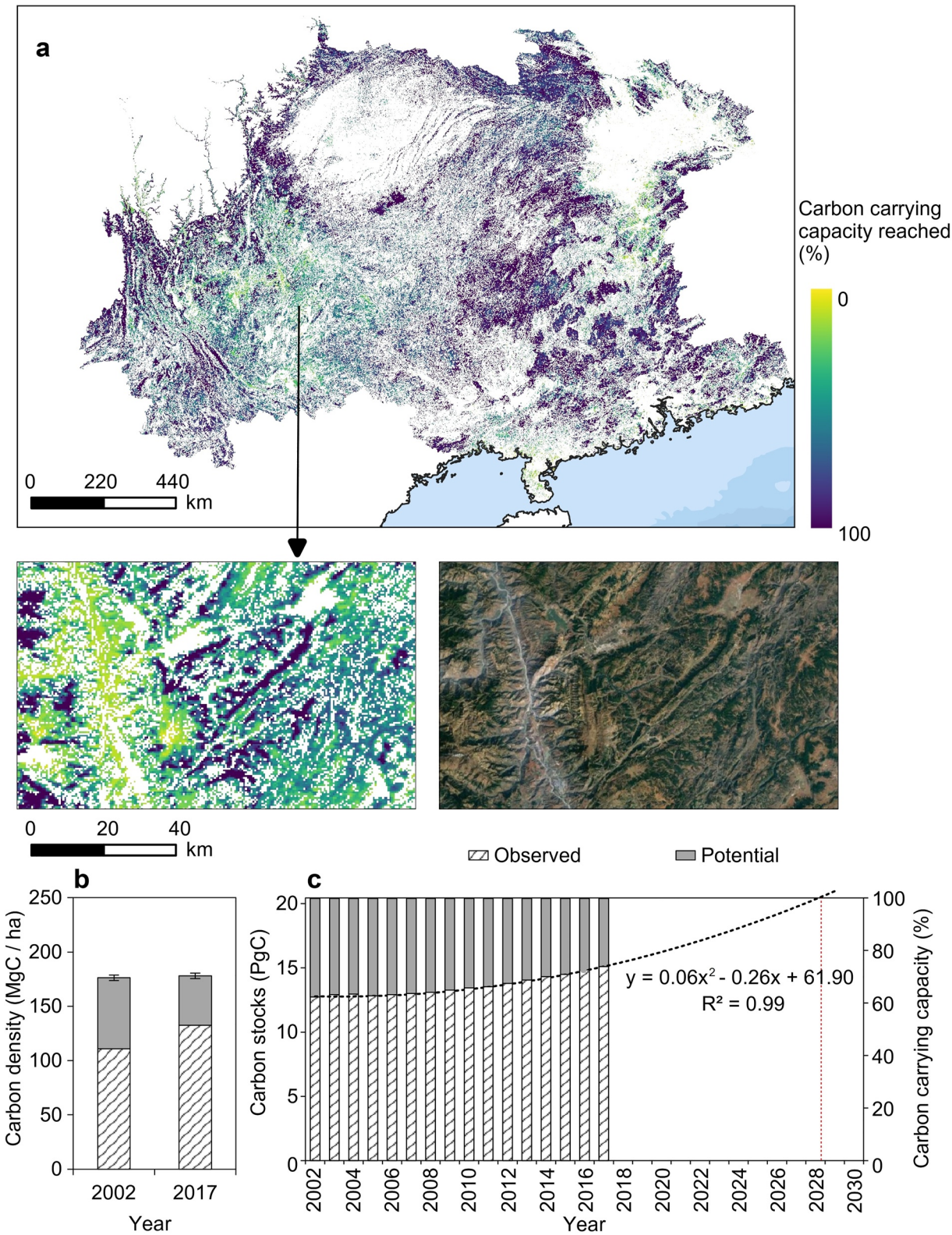

Figure 2. Carbon sink potential in the research area. (a) The % of the carbon carrying capacity that was reached in 2017. Croplands and urban areas are masked. The satellite image is from GoogleEarth. (b) Mean values of observed and potential carbon density in 2002 and 2017. The error bars reflect the differences between 5 model runs. (c) Observed and potential carbon stocks at annual scale. The right *y*-axis shows how much of the carrying capacity has been reached during 2002–2017. A polynomial regression was fitted over the annual data.

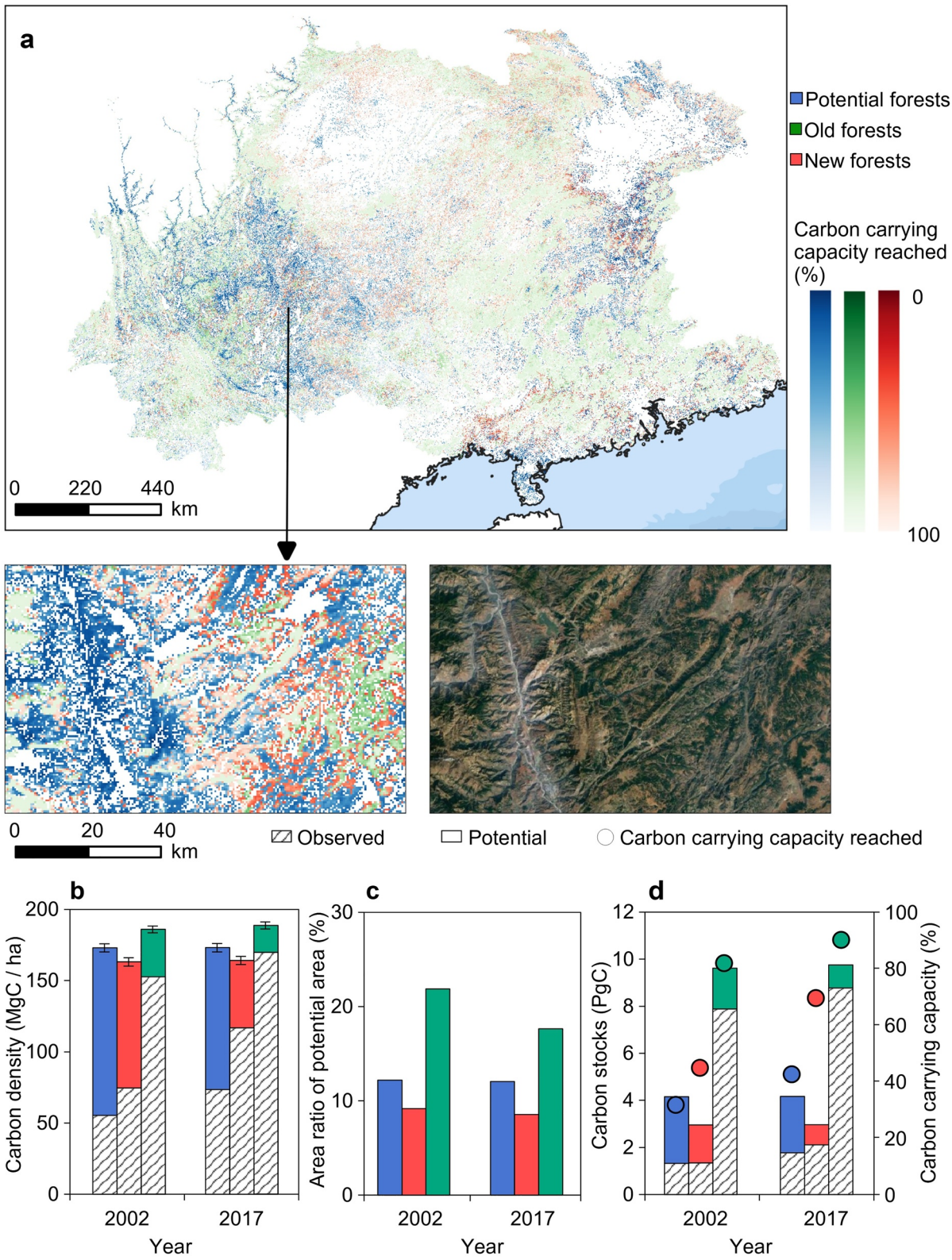

Figure 3. Potential carbon sequestration in different forest types. (a) The % of the carbon carrying capacity that was reached in different forest types in 2017. High values reflect a mature state of the vegetation. The satellite image is from GoogleEarth. (b) Mean values of observed and potential carbon density in different forest types in 2002 and 2017. The error bars reflect the differences between 5 model runs. (c) The proportion of areas with unsaturated carbon potential for different forest types in 2002 and 2017. (d) Potential carbon stocks and the percent of carrying capacity for different forest types in 2002 and 2017.

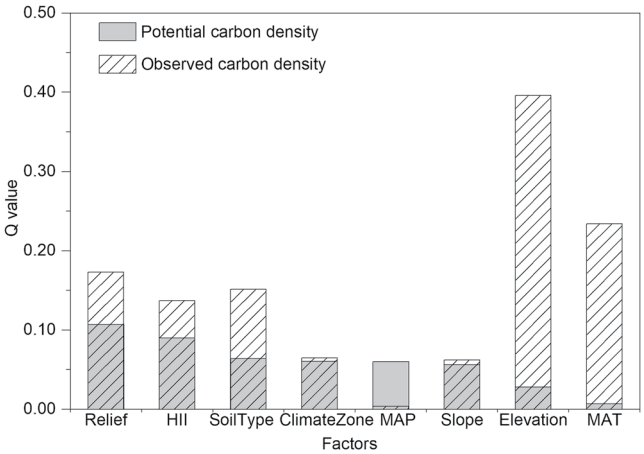

Figure 4. The relative importance of explanatory variables influencing the spatial pattern of carbon density. Relief: Terrain relief; HII: Human influence intensity; MAP: Mean annual precipitation; Elevation: Digital Elevation Model; MAT: Mean annual temperature.

The spatial patterns of potential, observed, and predicted (=carrying capacity) carbon density vary with factors, and we compared averaged carbon density for different stratums of each factor derived from the risk detector analysis (Figure 5) (Y. Z. Song et al., 2020). The potential carbon density clearly decreases with increasing terrain relief (Figure 5a) and increases with increasing human pressure (Figure 5b), while it is the opposite for the observed carbon density. Observed carbon density in rough (Figure 5a), remote (Figure 5b), and sloping (Figure 5f) areas was close to the carbon carrying capacity. The highest carbon carrying capacity and observed carbon density was found at an altitude between 2,500 m and 3,600 m (326.86 ± 7.03 and 263.72 MgC ha^{-1}) (Figure 5g), which coincides with the plateau climate zone (Figure 5d) characterized by low MAT and alfisols (Figure 5c). The highest average potential carbon density was found in areas with semi-alfisols controlled by southwest monsoon (Figures 5c and 5d). Potential carbon density showed a greater spatial difference for various levels of MAP as compared to MAT, and the areas with the highest carbon potential were located for areas with MAP less than 1,000 mm (Figure 5e) while fewer differences were found for different MAT levels (Figure 5h).

4. Discussion

4.1. A Win-Win Situation by Restoration Projects

Satellite based studies can only quantify aboveground carbon, but ignore soil carbon. Previous studies have shown that soil carbon is an important component of the total carbon stocks of karst ecosystems (Ni et al., 2015), and restoration projects in southern China did not only increase aboveground woody biomass but also had a documented positive impact on the soil carbon (Qin et al., 2022), which is not detected by our work. Promoting forest restoration and increasing tree cover to improve the above and belowground carbon stocks is a nature-based climate solution and a possible way to mitigate global climate change by removing CO_2 from the atmosphere (Doelman et al., 2020; Griscom et al., 2017). Therefore, local projects restoring forests and planting trees in karst areas are a crucial component of this pathway to sustainable carbon neutrality (Domke et al., 2020; Erbaugh et al., 2020; Wang et al., 2020). Over the past about two decades, afforestation and ecological restoration projects in southern China have transformed large areas of croplands into forests (Liao et al., 2018; Yue et al., 2020), with 5.32 PgC that can still be sequestered in form of aboveground woody biomass in 2017. Previous studies on this topic were mostly based on forest inventory plot data and rarely included new and potential forests. For example, Y. C. Liu et al. (2014) estimated the total carbon carrying capacity of China's forests using mature forests as reference level. They estimate the total carbon carrying capacity in southern China to be 7.90 PgC in 2006–2010, and the carbon sequestration potential 5.80 PgC. We estimate an aboveground carbon carrying capacity of 12.44 PgC for forests, with only 3.12 PgC sequestration potential in 2006. The difference can be explained by entirely different modeling approaches (interpolation between field plots vs. wall-to-wall remote sensing), different definitions of forest areas, and results may also be affected by the fact that optical satellite data saturate over old forests, underestimating their carrying capacity. The different numbers also show that soil carbon, which was excluded in our work, plays an important role (Achat et al., 2015). Future studies should combine both field plots and state-of-the-art remote sensing data and methods to reduce the uncertainty and harmonize estimations on potential carbon estimations such as presented here and by Y. C. Liu et al. (2014). The uncertainty may be less significant for new and potential forests, which are the major focus of this work, but there is currently a lack of comparable studies.

However, the rapid growth of trees limits the remaining carbon stock potential of the region, making regular carbon stock inventories an important part of forestation projects. Maximizing carbon uptake was not among the major aims when China's restoration projects were planned several decades ago. Rather poverty reduction, stopping the loss of top soil and rocky desertification as well as maximizing forest cover were key aims of the projects (Hua, Xu, & Wilcove, 2018; Jiang et al., 2014). The abandonment of croplands and the increase in forest cover can be regarded as environmental success, and our study shows that 73% of the carbon carrying capacity has been reached in 2017, which is 12% more than in 2002. The increase in carbon sequestration and other ecosystem

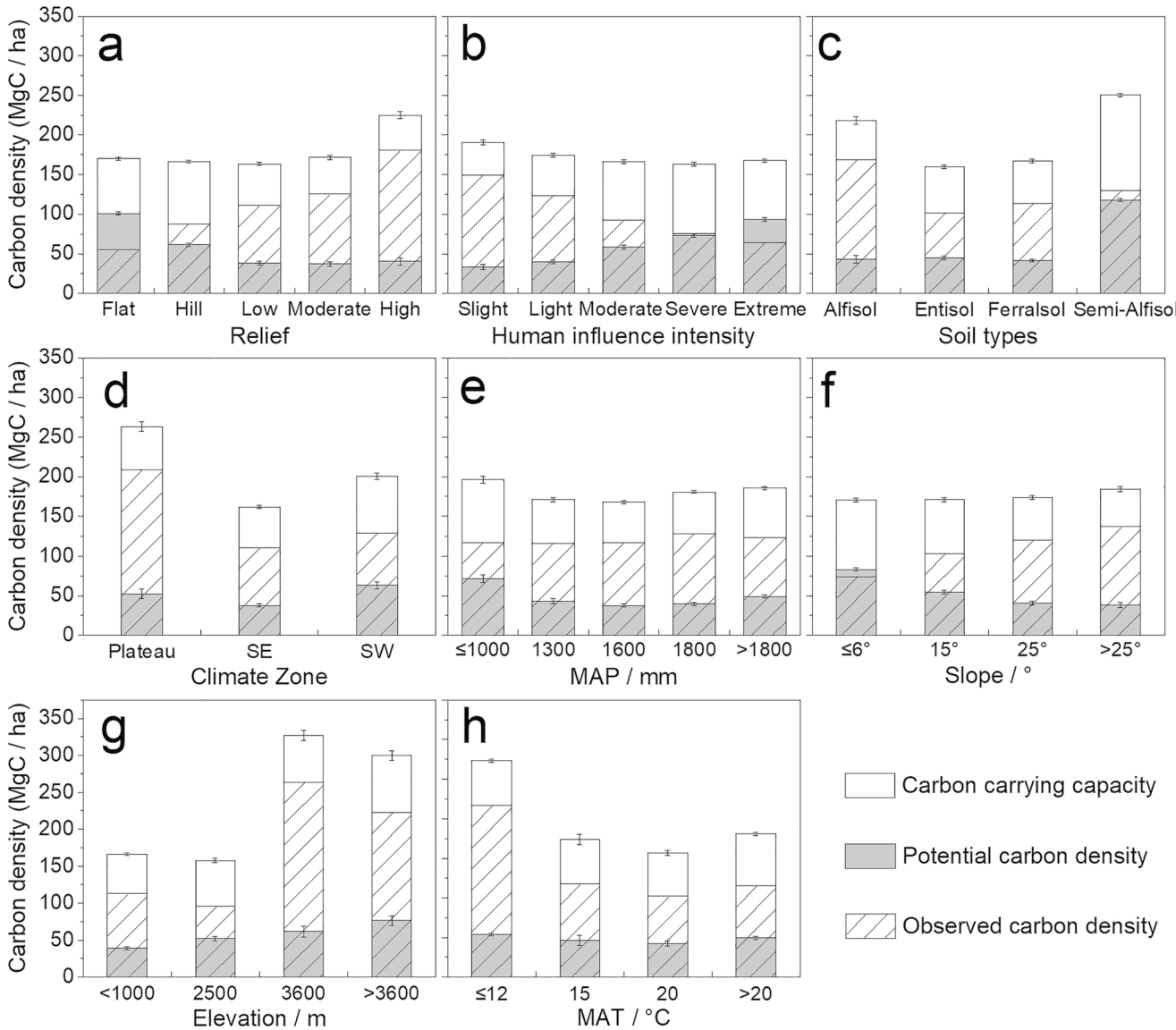

Figure 5. Average carbon density values for different classes of (a) relief (b) human influence intensity (c) soil types (d) climate zones (e) mean annual precipitation (MAP) (f) slope (g) elevation (Digital Elevation Model), and (h) mean annual temperature (MAT). Observed + potential carbon density = carbon carrying capacity.

services also benefits local livelihoods which is a win-win situation that not only addresses environmental problems and mitigates poverty, but also helps to combat climate change.

Our results uncover and quantify where vegetation has not yet reached its full potential, which is, not surprisingly, in non-forested areas, but also new forests which were planted in the frame of afforestation projects have only reached 71% of their potential in 2017, while old forests are close to their carbon carrying capacity (89%). A total of 58% of the remaining carbon stock potential is found in areas which are currently not forested mainly in the central of the Yunnan-Guizhou plateau, Nanling Mountains and the southeastern coastal areas of Guangdong. These areas should be the main target of future restoration programs, however, human interference, a harsh climate and fragile geological settings make a rapid recovery difficult (Wang et al., 2019; Yue et al., 2020). Potential forestation areas, include abandoned farmlands and mining areas, which are difficult to identify with coarse resolution imagery as used in this study, and require high-resolution images to precisely identify these areas.

Planted trees are usually selected based on the criteria of rapid growth and/or economic output, either by tree harvest or as cash crops. For example, fast growing *Eucalyptus* plantations rapidly generate revenues but do not

provide the same ecological benefits as native forests (Hua, Wang, et al., 2018). Moreover, most forest plantations are not optimized to sustain long-term carbon stocks (Palmer, 2021), which explains why only 10% of the region has reached its carbon carrying capacity, in spite of intensive forestation. Future ecological projects could be adjusted toward fixing more CO_2 maximizing the full carbon sequestration potential of the region.

Consequently, to improve future ecological projects and rapidly reach the full carbon sequestration potential of an area, it is crucial to identify the potential constraints of forest growth as well as determine the land available for sustainable afforestation (Waring et al., 2020), natural regeneration and assistant reconstruction (Palmer, 2021).

4.2. How to Make Full Use of the Local Carbon Carrying Capacity

We demonstrated that local terrain and human interference define the spatial patterns of vegetation carbon density in southern China, which differs from other studies conducted at national and global scale, highlighting the importance of climatic factors (Jiao et al., 2021), such as temperature and precipitation. For southern China, the subtropical monsoon climate provides sufficient rainfall, so human activities, such as economic development, urban expansion, agriculture, but also ecological restoration projects determine the patterns of forests (Lu et al., 2018). The spatial distribution of human population density is influenced by terrain (Ma & He, 2021), with human activities mainly being concentrated in areas of low elevation, and flat terrain. We observed that observed and potential carbon density varied with the intensity of human interference and terrain (Figure S4 in Supporting Information S2), and their interaction showed a synergistic effect on the spatial pattern of aboveground biomass (Table S6 in Supporting Information S3) and carbon sequestration potential (Table S7 in Supporting Information S3), which can be interpreted by the following points. First, many croplands have been transformed into managed forests dominated by monocultures with a high remaining carbon sequestration potential. Second, native forests close to croplands and urban areas have often been replaced by afforestation areas yielding higher economic output, resulting in a decline of ecological benefits, such as biodiversity, carbon sequestration and water retention (Hua, Wang, et al., 2018, Hua, Xu, & Wilcove, 2018; Ouyang et al., 2016). These areas usually have favorable natural conditions and efforts replacing monocultures with multiple species or assist natural regeneration could generate a potential carbon sink (Lamb et al., 2005). Also, bare areas resulting from construction and mining works have a certain carbon sink potential (Wang et al., 2018), but the restoration of these areas is challenging. Forests in protected areas with little human interference (NDRC, 2016) as well as forests in remote mountain areas (López-Pujol et al., 2011) are less disturbed and close to their carrying capacity with a lower carbon sequestration potential.

Soil types are important as well, and we found a higher observed carbon density and carbon carrying capacity in areas with alfisol soils. These areas are mostly in high elevation mountains, and more than 25% of this area has reached its carbon carrying capacity, which also indicates that less human interference is an important factor for reaching carbon carrying capacity. A higher carbon sink potential was found in dry red soil, one class of semi-alfisols (Shi et al., 2010; Zhang et al., 2003), which are mainly distributed in dry-hot valleys of the Hengduan Mountains. Plant growth in these areas is controlled by a special climate with high temperature and low rainfall (F. Y. Liu et al., 2010; Yang et al., 2016), which leads to a lower carbon carrying capacity compared with the valleys in high elevation. Moreover, native tropical valley monsoon forests have been degraded from human overuse and are difficult to recover in this dry area (Ma & McConchie, 2001), consequently, almost no aboveground biomass was observed. Here, vegetation communities vary with elevation and slope (He et al., 2000), which requires adjusted ecological restoration measures according to different situations (Zhang et al., 2003). For example, tropical and subtropical economic fruit species could be introduced into this area with better water conservancy conditions (HKT, 2021), while water-deficient areas are suitable for introducing drought tolerant savanna woody species (Zhang et al., 2012), which would not only improve the region's economy, but also increase carbon sequestration.

In summary, the carbon sink potential in areas with a high human pressure and steep slope is still high. These areas have now been located and their potential has been quantified, it is now up to stakeholders to take action.

5. Conclusions

Forestation programs have been suggested as a measure to mitigate global climate change. southern China has been subject to large-scale forestation activities over the past about two decades, but the longevity of this carbon sink is rather unknown. We find that 8% of the area has been forested during 2002–2017, consuming 12% of the carbon carrying capacity over the past about two decades. This implies that the region has reached 73% of the carbon carrying capacity in 2017. However, previous forestation projects were designed to maximize forest cover but not carbon stocks, and future forestation programs need to make use of maps such as the one provided by this study to identify areas that are below their carbon carrying capacity. Moreover, planted tree species, tree density and harvest cycles can be adjusted to generate a long-term and sustainable carbon sink making use of the local carbon carrying capacity of a given area. However, we also show that afforestation provides only a short-term solution as climate change mitigation measure and only a reduction of CO_2 emissions can mitigate climate change in the long term.

Data Availability Statement

Our maps are available from https://doi.org/10.5281/zenodo.7146104. Roadmap in shapefile format can be downloaded at https://download.geofabrik.de/asia.html, nighttime lights at https://dataverse.harvard.edu/dataset.xhtml?persistentId=doi:10.7910/DVN/YGIVCD, and land use types data at http://www.globeland30.org/defaults_en.html?src=/Scripts/map/defaults/En/download_en.html%26head=download%26type=data. The Random Forest model was run in a GRASS GIS environment with the r.randomforest package (https://cran.r-project.org/web/packages/randomForest/). The OPGD model was run with the r.GD package (https://cran.r-project.org/web/packages/GD/vignettes/GD.html).

Acknowledgments
This study was funded by the National Key Research and Development Program of China (2022YFF1300700, 2018YFD1100103), the National Natural Science Foundation of China (41930652, U20A2048); the Marie Curie fellowship (795970), the CAS Interdisciplinary Innovation Team (JCTD-2021-16) and the China Scholarship Council (CSC202004910531). M.B. received funding from the DFF Sapere Aude (9064-00049B) and the European Research Council (ERC) under the European Union's Horizon 2020 Research and Innovation Programme (grant agreement no. 947757 TOFDRY). We thank http://www.naturalearthdata.com for providing background maps.

References

Achat, D. L., Fortin, M., Landmann, G., Ringeval, B., & Augusto, L. (2015). Forest soil carbon is threatened by intensive biomass harvesting. *Scientific Reports*, *5*(1), 15991. https://doi.org/10.1038/srep15991

Benítez, P. C., McCallum, I., Obersteiner, M., & Yamagata, Y. (2007). Global potential for carbon sequestration: Geographical distribution, country risk and policy implications. *Ecological Economics*, *60*(3), 572–583. https://doi.org/10.1016/j.ecolecon.2005.12.015

Brandt, M., Yue, Y. M., Wigneron, J. P., Tong, X. W., Tian, F., Jepsen, M. R., et al. (2018). Satellite-observed major greening and biomass increase in South China karst during recent decade. *Earth's Future*, *6*(7), 1017–1028. https://doi.org/10.1029/2018ef000890

Cai, W. X., He, N. P., Li, M. X., Xu, L., Wang, L. Z., Zhu, J. H., et al. (2021). Carbon sequestration of Chinese forests from 2010–2060: Spatiotemporal dynamics and its regulatory strategies. *Science Bulletin*, *67*(8), 836–843. https://doi.org/10.1016/j.scib.2021.12.012

Chen, Z. Q., Yu, B. L., Yang, C. S., Zhou, Y. Y., Yao, S. J., Qian, X. J., et al. (2020). An extended time-series (2000–2018) of global NPP-VIIRS-like nighttime light data. https://doi.org/10.7910/DVN/YGIVCD

Cheng, W. M., & Zhou, C. H. (2014). *Geomorphological of China 1:4,000,000*. In National Tibetan Plateau data (Ed.), National Tibetan Plateau Data Center. https://doi.org/10.11888/Geogra.tpdc.270602

China Meteorological Administration (CMA). (1978). Climate regionalization in China. Retrieved from https://www.resdc.cn/data.aspx?dataid=243

Cook-Patton, S. C., Leavitt, S. M., Gibbs, D., Harris, N. L., Lister, K., Anderson-Teixeira, K. J., et al. (2020). Mapping carbon accumulation potential from global natural forest regrowth. *Nature*, *585*(7826), 545–550. https://doi.org/10.1038/s41586-020-2686-x

Doelman, J. C., Stehfest, E., van Vuuren, D. P., Tabeau, A., Hof, A. F., Braakhekke, M. C., et al. (2020). Afforestation for climate change mitigation: Potentials, risks and trade-offs. *Global Change Biology*, *26*(3), 1576–1591. https://doi.org/10.1111/gcb.14887

Domke, G. M., Oswalt, S. N., Walters, B. F., & Morin, R. S. (2020). Tree planting has the potential to increase carbon sequestration capacity of forests in the United States. *Proceedings of the National Academy of Sciences*, *117*(40), 24649–24651. https://doi.org/10.1073/pnas.2010840117

Erbaugh, J. T., Pradhan, N., Adams, J., Oldekop, J. A., Agrawal, A., Brockington, D., et al. (2020). Global forest restoration and the importance of prioritizing local communities. *Nature Ecology & Evolution*, *4*(11), 1472–1476. https://doi.org/10.1038/s41559-020-01282-2

Fang, J., Yu, G., Liu, L., Hu, S., & Chapin, F. S. (2018). Climate change, human impacts, and carbon sequestration in China. *Proceedings of the National Academy of Sciences*, *115*(16), 4015–4020. https://doi.org/10.1073/pnas.1700304115

FAO. (2020). Global forest Resources assessment 2020—key findings. https://doi.org/10.4060/ca8753en

Griscom, B. W., Adams, J., Ellis, P. W., Houghton, R. A., Lomax, G., Miteva, D. A., et al. (2017). Natural climate solutions. *Proceedings of the National Academy of Sciences*, *114*(44), 11645–11650. https://doi.org/10.1073/pnas.1710465114

Hamilton, S. E., & Friess, D. A. (2018). Global carbon stocks and potential emissions due to mangrove deforestation from 2000 to 2012. *Nature Climate Change*, *8*(3), 240–244. https://doi.org/10.1038/s41558-018-0090-4

He, N. P., Wen, D., Zhu, J. X., Tang, X. L., Xu, L., Zhang, L., et al. (2017). Vegetation carbon sequestration in Chinese forests from 2010 to 2050. *Global Change Biology*, *23*(4), 1575–1584. https://doi.org/10.1111/gcb.13479

He, Y. B., Lu, P. Z., & Zhu, T. (2000). Causes for the formation of dry-hot valleys in Hengduan mountain–Yunnan Plateau. *Resources Science*, *22*, 69–72.

Heinrich, V. H., Dalagnol, R., Cassol, H. L., Rosan, T. M., de Almeida, C. T., Junior, C. S., et al. (2021). Large carbon sink potential of secondary forests in the Brazilian Amazon to mitigate climate change. *Nature Communications*, *12*, 1–11. https://doi.org/10.1038/s41467-021-22050-1

HKT. (2021). Dry and hot valley: A special microclimate that breaks the boundaries of plant growth. *iNEWS, Nature*. Retrieved from https://inf.news/en/nature/0c5487c3eaaf453d6156a5dc78f3e113.html

Houghton, R. A. (2008). *Biomass. Encyclopaedia Ecology* (pp. 448–453). Elsevier. https://doi.org/10.1016/B978-008045405-4.00462-6
Hua, F. Y., Xu, J. C., & Wilcove, D. S. (2018). A new opportunity to recover native forests in China. *Conservation Letters*, *11*(2), e12396. https://doi.org/10.1111/conl.12396
Hua, F. Y., Wang, L., Fisher, B., Zheng, X. L., Wang, X. Y., Yu, D. W., et al. (2018). Tree plantations displacing native forests: The nature and drivers of apparent forest recovery on former croplands in Southwestern China from 2000 to 2015. *Biological Conservation*, *222*, 113–124. https://doi.org/10.1016/j.biocon.2018.03.034
IPCC. (2001). Impacts, adaptation, a TAR climate change 2001: Impacts, adaptation, and vulnerability. Retrieved from https://www.ch/report/ar3/wg2
Jiang, Z. C., Lian, Y. Q., & Qin, X. Q. (2014). Rocky desertification in Southwest China: Impacts, causes, and restoration. *Earth-Science Reviews*, *132*, 1–12. https://doi.org/10.1016/j.earscirev.2014.01.005
Jiao, W. Z., Wang, L. X., Smith, W. K., Chang, Q., Wang, H. L., & D'Odorico, P. (2021). Observed increasing water constraint on vegetation growth over the last three decades. *Nature Communications*, *12*(1), 3777. https://doi.org/10.1038/s41467-021-24016-9
Keith, H., Mackey, B., Berry, S., Lindenmayer, D., & Gibbons, P. (2010). Estimating carbon carrying capacity in natural forest ecosystems across heterogeneous landscapes: Addressing sources of error. *Global Change Biology*, *16*, 2971–2989. https://doi.org/10.1111/j.1365-2486.2009.02146.x
Kumar, B. (2006). *Carbon sequestration potential of tropical homegardens. Tropical Homegardens* (pp. 185–204). Springer. https://doi.org/10.1007/978-1-4020-4948-4_11
Lal, M., & Singh, R. (2000). Carbon sequestration potential of Indian forests. *Environmental Monitoring and Assessment*, *60*(3), 315–327. https://doi.org/10.1023/a:1006139418804
Lamb, D., Erskine Peter, D., & Parrotta John, A. (2005). Restoration of degraded Tropical forest landscapes. *Science*, *310*(5754), 1628–1632. https://doi.org/10.1126/science.1111773
Li, B. Y., Pan, B. T., & Han, J. F. (2008). Basic terrestrial geomorphological types in China and their circumscriptions. *Quaternary Sciences*, *28*(4), 535–543.
Li, S. C., Zhang, Y. L., Wang, Z. F., & Li, L. H. (2018). Mapping human influence intensity in the Tibetan Plateau for conservation of ecological service functions. *Ecosystem Services*, *30*, 276–286. https://doi.org/10.1016/j.agrformet.2018.02.015
Liao, C. J., Yue, Y. M., Wang, K. L., Fensholt, R., Tong, X. W., & Brandt, M. (2018). Ecological restoration enhances ecosystem health in the karst regions of southwest China. *Ecological Indicators*, *90*, 416–425. https://doi.org/10.1016/j.ecolind.2018.03.036
Liu, F. Y., Li, K., Sun, Y. Y., Tang, G. Y., & Zhang, C. H. (2010). Effects of climate on vegetation recovery in dry-hot valleys of Hengduan Mountains region in southern China. *Resources and Environment in the Yangtze Basin*, *19*, 1386–1391.
Liu, H. Y., Jiao, F. S., Yin, J. Q., Li, T. Y., Gong, H. B., Wang, Z. Y., & Lin, Z. S. (2020). Nonlinear relationship of vegetation greening with nature and human factors and its forecast—A case study of Southwest China. *Ecological Indicators*, *111*, 12. https://doi.org/10.1016/j.ecolind.2019.106009
Liu, Y. C., Yu, G. R., Wang, Q. F., Zhang, Y. J., & Xu, Z. H. (2014). Carbon carry capacity and carbon sequestration potential in China based on an integrated analysis of mature forest biomass. *Science China Life Sciences*, *57*(12), 1218–1229. https://doi.org/10.1007/s11427-014-4776-1
López-Pujol, J., Zhang, F. M., Sun, H. Q., Ying, T. S., & Ge, S. (2011). Mountains of southern China as "plant museums" and "plant cradles": Evolutionary and conservation insights. *Mountain Research and Development*, *31*(3), 261–269. https://doi.org/10.1659/MRD-JOURNAL-D-11-00058.1
Lu, F., Hu, H. F., Sun, W. J., Zhu, J. J., Liu, G. B., Zhou, W. M., et al. (2018). Effects of national ecological restoration projects on carbon sequestration in China from 2001 to 2010. *Proceedings of the National Academy of Sciences*, *115*(16), 4039–4044. https://doi.org/10.1073/pnas.1700294115
Lv, Y., Hu, J., Fu, B., Harris, P., Wu, L., Tong, X., et al. (2019). A framework for the regional critical zone classification: The case of the Chinese Loess Plateau. *National Science Review*, *6*(1), 14–18. https://doi.org/10.1093/nsr/nwy147
Ma, C., & He, Y. (2021). Spatiotemporal trends and ecological determinants in population by elevation in China since 1990. *Chinese Geographical Science*, *31*(2), 248–260. https://doi.org/10.1007/s11769-021-1188-6
Ma, H. C., & McConchie, J. A. (2001). The dry-hot valleys and forestation in southwest China. *Journal of Forestry Research*, *12*(1), 35–39. https://doi.org/10.1007/BF02856797
Macreadie, P. I., Ollivier, Q. R., Kelleway, J. J., Serrano, O., Carnell, P. E., Ewers Lewis, C. J., et al. (2017). Carbon sequestration by Australian tidal marshes. *Scientific Reports*, *7*(1), 44071. https://doi.org/10.1038/srep44071
National Development and Reform Commission (NDRC)People's Republic of China. (2016). The 13th five-year construction Plan for the comprehensive control Project of rocky desertification in karst areas (pp. 17–18).
Nguyen, K. A., & Liou, Y. A. (2019). Global mapping of eco-environmental vulnerability from human and nature disturbances. *Science of The Total Environment*, *664*, 995–1004. https://doi.org/10.1016/j.scitotenv.2019.01.407
Ni, J., Luo, D. H., Xia, J., Zhang, Z. H., & Hu, G. (2015). Vegetation in karst terrain of southwestern China allocates more biomass to roots. *Solid Earth*, *6*(3), 799–810. https://doi.org/10.5194/se-6-799-2015
Nunes, L. J. R., Meireles, C. I. R., Pinto Gomes, C. J., & Almeida Ribeiro, N. M. C. (2020). Forest contribution to climate change mitigation: Management oriented to carbon capture and storage. *Climate*, *8*(2), 21. https://doi.org/10.3390/cli8020021
Ouyang, Z. Y., Zheng, H., Xiao, Y., Polasky, S., Liu, J. G., Xu, W. H., et al. (2016). Improvements in ecosystem services from investments in natural capital. *Science*, *352*(6292), 1455–1459. https://doi.org/10.1126/science.aaf2295
Palmer, L. (2021). How trees and forests reduce risks from climate change. *Nature Climate Change*, *11*(5), 374–377. https://doi.org/10.1038/s41558-021-01041-6
Pang, J. F., Ding, X. Z., Han, K. Y., Zeng, Y., Chen, A. S., Zhang, Y. L., et al. (2017). 1:1000,000 spatial database of national digital geological map. *China geology*, *44*(S1), 8–18.
Pascual, A., Giardina, C. P., Selmants, P. C., Laramee, L. J., & Asner, G. P. (2021). A new remote sensing-based carbon sequestration potential index (CSPI): A tool to support land carbon management. *Forest Ecology and Management*, *494*, 119343. https://doi.org/10.1016/j.foreco.2021.119343
Piao, S., Yin, G., Tan, J., Cheng, L., Huang, M., Li, Y., et al. (2015). Detection and attribution of vegetation greening trend in China over the last 30 years. *Global Change Biology*, *21*(4), 1601–1609. https://doi.org/10.1111/gcb.12795
Qin, C., Li, S. L., Yu, G. H., Bass, A. M., Yue, F. J., & Xu, S. (2022). Vertical variations of soil carbon under different land uses in a karst critical zone observatory (CZO), SW China. *Geoderma*, *412*, 115741. https://doi.org/10.1016/j.geoderma.2022.115741
Reichstein, M., Bahn, M., Ciais, P., Frank, D., Mahecha, M. D., Seneviratne, S. I., et al. (2013). Climate extremes and the carbon cycle. *Nature*, *500*(7462), 287–295. https://doi.org/10.1038/nature12350
Ross, C. W., Hanan, N. P., Prihodko, L., Anchang, J., Ji, W. J., & Yu, Q. Y. (2021). Woody-biomass projections and drivers of change in sub-Saharan Africa. *Nature Climate Change*, *11*(5), 449–455. https://doi.org/10.1038/s41558-021-01034-5

Roxburgh, S. H., Wood, S. W., Mackey, B. G., Woldendorp, G., & Gibbons, P. (2006). Assessing the carbon sequestration potential of managed forests: A case study from temperate Australia. *Journal of Applied Ecology*, *43*(6), 1149–1159. https://doi.org/10.1111/j.1365-2664.2006.01221.x

Sanderson, E. W., Jaiteh, M., Levy, M. A., Redford, K. H., Wannebo, A. V., & Woolmer, G. (2002). The human footprint and the last of the wild. *BioScience*, *52*(10), 891–904. https://doi.org/10.1641/0006-3568(2002)052[0891:THFATL]2.0.CO;2

SFGA. (2021). Bulletin on China's land greening in 2020. State forestry and grassland administration. Retrieved from http://www.forestry.gov.cn/main/393/20210312/175043478886085.html

Shi, X. Z., Yu, D. S., Xu, S. X., Warner, E. D., Wang, H. J., Sun, W. X., et al. (2010). Cross-reference for relating genetic soil classification of China with WRB at different scales. *Geoderma*, *155*(3–4), 344–350. https://doi.org/10.1016/j.geoderma.2009.12.017

Song, X. D., Yang, F., Wu, H. Y., Zhang, J., Li, D. C., Liu, F., et al. (2021). Significant loss of soil inorganic carbon at the continental scale. *National Science Review*, *9*(2). https://doi.org/10.1093/nsr/nwab120

Song, Y. Z., Wang, J. F., Ge, Y., & Xu, C. D. (2020). An optimal parameters-based geographical detector model enhances geographic characteristics of explanatory variables for spatial heterogeneity analysis: Cases with different types of spatial data. *GIScience and Remote Sensing*, *57*(5), 593–610. https://doi.org/10.1080/15481603.2020.1760434

Tang, X., Zhao, X., Bai, Y., Tang, Z. Y., Wang, W. T., Zhao, Y. C., et al. (2018). Carbon pools in China's terrestrial ecosystems: New estimates based on an intensive field survey. *Proceedings of the National Academy of Sciences*, *115*(16), 4021–4026. https://doi.org/10.1073/pnas.1700291115

Tong, X., Brandt, M., Yue, Y., Ciais, P., Rudbeck, J. M., Penuelas, J., et al. (2020). Forest management in southern China generates short term extensive carbon sequestration. *Nature Communications*, *11*(1), 129. https://doi.org/10.1038/s41467-019-13798-8

Tong, X., Brandt, M., Yue, Y., Horion, S., Wang, K. L., Keersmaecker, W. D., et al. (2018). Increased vegetation growth and carbon stock in China karst via ecological engineering. *Nature Sustainability*, *1*, 44–50. https://doi.org/10.1038/s41893-017-0004-x

Udawatta, R. P., & Jose, S. (2011). Carbon sequestration potential of agroforestry systems. *Advances in Agroforestry*, *8*, 17–42. https://doi.org/10.1007/978-94-007-1630-8_2

Wang, H., Zhang, B., Bai, X., & Shi, L. (2018). A novel environmental restoration method for an abandoned limestone quarry with a deep open pit and steep palisades: A case study. *Royal Society Open Science*, *5*, 180365. https://doi.org/10.1098/rsos.180365

Wang, J., Feng, L., Palmer, P. I., Liu, Y., Fang, S. X., Bösch, H., et al. (2020). Large Chinese land carbon sink estimated from atmospheric carbon dioxide data. *Nature*, *586*(7831), 720–723. https://doi.org/10.1038/s41586-020-2849-9

Wang, J. F., & Xu, C. D. (2017). Geodetector: Principle and prospective. *Acta Geographica Sinica*, *72*(1), 116–134. https://doi.org/10.11821/dlxb201701010

Wang, K. L., Zhang, C. H., Chen, H. S., Yue, Y. M., Zhang, W., Zhang, M. Y., et al. (2019). Karst landscapes of China: Patterns, ecosystem processes and services. *Landscape Ecology*, *34*(12), 2743–2763. https://doi.org/10.1007/s10980-019-00912-w

Wang, S., Zhou, L., Chen, J., Ju, W. M., Feng, X. F., & Wu, W. X. (2011). Relationships between net primary productivity and stand age for several forest types and their influence on China's carbon balance. *Journal of Environmental Management*, *92*(6), 1651–1662. https://doi.org/10.1016/j.jenvman.2011.01.024

Waring, B., Neumann, M., Prentice, I. C., Adams, M., Smith, P., & Siegert, M. (2020). *What role can forests play in tackling climate change?* Imperial College London.

Wu, G. L., Cheng, Z., Alatalo, J. M., Zhao, J. X., & Liu, Y. (2021). Climate warming consistently reduces grassland ecosystem productivity. *Earth's Future*, *9*(6), e2020EF001837. https://doi.org/10.1029/2020EF001837

Yang, J. D., Zhang, Z. M., Shen, Z. H., Ou, X. K., Geng, Y. P., & Yang, M. Y. (2016). Review of research on the vegetation and environment of dry-hot valleys in Yunnan. *Biodiversity Science*, *24*(4), 462–474. https://doi.org/10.17520/biods.2015251

Yu, Y., Chen, J. M., Yang, X., Fan, W., Fan, W. Y., Li, M. Z., & He, L. M. (2017). Influence of site index on the relationship between forest net primary productivity and stand age. *PLoS One*, *12*(5), e0177084. https://doi.org/10.1371/journal.pone.0177084

Yue, Y. M., Liao, C. J., Tong, X. W., Wu, Z. B., Fensholt, R., Prishchepov, A., et al. (2020). Large scale reforestation of farmlands on sloping hills in South China karst. *Landscape Ecology*, *35*(6), 1445–1458. https://doi.org/10.1007/s10980-020-01026-4

Zhang, D. N., Zuo, X. X., & Zang, C. F. (2021). Assessment of future potential carbon sequestration and water consumption in the construction area of the Three-North Shelterbelt Programme in China. *Agricultural and Forest Meteorology*, *303*, 108377. https://doi.org/10.1016/j.agrformet.2021.108377

Zhang, J. L., Poorter, L., & Cao, K. F. (2012). Productive leaf functional traits of Chinese savanna species. *Plant Ecology*, *213*(9), 1449–1460. https://doi.org/10.1007/s11258-012-0103-8

Zhang, X. B., Yang, Z., & Zhang, J. P. (2003). Lithologic types on hill slopes and revegetation zoning in the Yuanmou hot and dry valley. *Scientia Silvae Sinicae*, *39*, 16–22. https://doi.org/10.11707/j.1001-7488.20030403

Zhang, X. M., Yue, Y. M., Tong, X. W., Wang, K. L., Qi, X. K., Deng, C. Q., & Brandt, M. (2021). Eco-engineering controls vegetation trends in southwest China karst. *Science of The Total Environment*, *770*, 145160. https://doi.org/10.1016/j.scitotenv.2021.145160

Zhang, Y., Yao, Y., Wang, X., Liu, Y., & Piao, S. (2017). Mapping spatial distribution of forest age in China. *Earth and Space Science*, *4*(3), 108–116. https://doi.org/10.1002/2016EA000177

Zhao, S., Pereira, P., Wu, X. Q., Zhou, J. X., Cao, J. H., & Zhang, W. X. (2020). Global karst vegetation regime and its response to climate change and human activities. *Ecological Indicators*, *113*, 11. https://doi.org/10.1016/j.ecolind.2020.106208